Microskeletal Structures Suggest Taxonomic Distinction between Subgenera of Azooxanthellate Scleractinian Flabellum

Authors: Tokuda, Yuki, and Ezaki, Yoichi

Source: Paleontological Research, 24(4) : 261-275

Published By: The Palaeontological Society of Japan

URL: https://doi.org/10.2517/2019PR021

Paleontological Research, vol. 24, no. 4, pp. 261–275, October 1, 2020

doi:10.2517/2019PR021

Microskeletal structures suggest taxonomic distinction between subgenera of azooxanthellate scleractinian *Flabellum*

YUKI TOKUDA[1] AND YOICHI EZAKI[2]

[1]*Tottori University of Environmental Studies, 1-1-1 Wakabadaikita, Tottori 689-1111, Japan (e-mail: tokuda35@gmail.com)*
[2]*Department of Geosciences, Graduate School of Science, Osaka City University, 3-3-138 Sugimoto, Sumiyoshi-ku, Osaka 558-8585, Japan*

Received March 31, 2018; Revised manuscript accepted October 17, 2019

Abstract. Recent molecular analyses have challenged the traditional classification of scleractinian corals at almost all taxonomic levels, suggesting a requirement of new morphological characters for classification. Microskeletal characters have shown great potential to support the classification of the molecular-based clades of the scleractinian corals. *Flabellum* (Family Flabellidae) is the fifth largest genus and contains two subgenera, *F.* (*Flabellum*) and *F.* (*Ulocyathus*). The genus is very important in deciphering flabellid evolution, as phylogenetic relationship is still ambiguous in this family. In particular, little is known of the microstructural features of *Flabellum* species. Here we discuss the microskeletal structures of *F.* (*F.*) *magnificum* and *F.* (*U.*) *deludens*. Rapid accretion deposits (RADs) on the walls of *F.* (*F.*) *magnificum* show dome-shaped strands *ca.* 50–100 μm wide, which are composed alternatively of microcrystalline and fibrous parts. In contrast, the RADs on the walls of *F.* (*U.*) *deludens* consist of strands (50–100 μm long and 20–30 μm wide) made up of very short fibers (*ca.* 0.5–5 μm long) or microcrystallines with meniscus structure and dome-shaped fibrous layers. Thickening deposits (TDs) on the walls of both species are characterized by three qualities: (1) layered bundles consisting of fibrous crystals; (2) shingle-like TDs composed of small crystals and microcrystallines; and (3) shingle-like TDs comprised of larger fibers. In particular, in *F.* (*U.*) *deludens*, the TD of the calicular side of the wall is mainly formed of shingle-like TDs. The walls of *F.* (*U.*) *deludens* and *F.* (*F.*) *magnificum* thus differ completely in terms of the RAD (digitated strand and dome-shaped fibrous layers vs. continuous dome-shaped alternation) and TD characteristics. These kinds of microskeletal differences could support the molecular phylogenetic distinction between the *F.* (*U.*) spp. cluster and the *F.* (*F.*) clusters.

Key words: azooxanthellate corals, biomineralization, Flabellidae, Scleractinia, taxonomy

Introduction

The family Flabellidae Bourne, 1905 (Cnidaria: Scleractinia) comprises 14 exclusively solitary and azooxanthellate genera and is the fifth species-richest family among the 24 families containing extant species in the Scleractinia (Cairns, 1999, 2017). These corals are widely distributed in depths ranging from 0 m to 3186 m, exhibiting specific life modes and morphologies (Cairns, 2017).

The coralla of genus *Flabellum* contain ceratoid, campanulate, bowl-shaped, discoidal, or compressed flabellate without pali, dissepiments, and synapticulae. *Flabellum* contains two subgenera: *F.* (*Flabellum*) characterized by a smooth calicular margin and *F.* (*Ulocyathus*) distinguished by a serrate or jagged calicular margin (Cairns, 1989). *F.* (*Flabellum*) contains 25 Recent species, whereas *F.* (*Ulocyathus*) consists of 19, for a total of 44 Recent species (Cairns, 2016). *Flabellum* is the fifth largest genus by number of species, among the ~240 extant scleractinian genera (Cairns, 2016). The genus is also known from ~144 nominal fossil species recorded from as early as the late Cretaceous (Cairns, 2016).

However, the phylogenetic relationship among the flabellids is still ambiguous. Recently, molecular phylogenetic analyses have been performed on Scleractinia. The suggested phylogenetic relationships differ from the traditional ones based mainly on skeletal morphologies (Romano and Palumbi, 1996; Romano and Cairns, 2000; Fukami *et al.*, 2004; Le Goff-Vitry *et al.*, 2004; Fukami *et al.*, 2008; Kitahara *et al.*, 2010; Stolarski *et al.*, 2011). As such, the traditional systematic relationships require revision based on this new molecular phylogenetic evidence, suggesting the need to analyze new morphological characters for classification. Microskeletal characters have shown great potential to support the classification of molecular-based clades of the scleractinian corals (Cuif *et al.*, 2003; Benzoni *et al.*, 2007; Budd and Stolarski, 2009; Benzoni *et al.*, 2012; Kitahara *et al.*, 2012). Romano and Cairns (2000); Le Goff-Vitry *et al.* (2004); Kitahara *et al.* (2010); Tokuda *et al.* (2010), and Stolarski *et al.* (2011) have conducted molecular phylogenetic analyses on some flabellids. However, detailed phylogenetic relationships in the Flabellidae remain mostly unelucidated. The genus *Flabellum* is polyphyletic in origin (Kitahara *et al.*, 2010; Tokuda *et al.*, 2010; Stolarski *et al.*, 2011). Skeletal microstructures of flabellid corals have been studied by Sorauf and Podoff (1977), and Stolarski (1995, 1996, 2003). In particular, Stolarski (2003) described various microscopic characteristics of *F.* (*F.*) *chunii* Marenzeller, 1904. However, similar microstructural details of other flabellids remain unknown. Particularly, little is known of the microstructural features of *F.* (*Ulocyathus*) species. Microskeletal structures of *Flabellum* species are therefore investigated to define and delimit a new set of morphological characters that reflect skeletal growth, and to determine the correlation between these characters and molecular phylogenetic data. Additionally, we investigate how microstructures play essential roles in the formation of macromorphologies.

Materials and methods

Specimens of *Flabellum* (*Flabellum*) *magnificum* and *Flabellum* (*Ulocyathus*) *deludens* were collected off Makurazaki, Kagoshima Prefecture, Japan (from a depth of ~300 m). The terminology of skeletal microstructural characteristics follows that of Stolarski (2003), Brahmi *et al.* (2010), and Janiszewska *et al.* (2011). In scleractinian corals, two essential skeletal structures are observed at the microscopic level; they are traditionally referred to as the centers of calcification (COC) and fibers (e.g. Bourne, 1887; Oglivie, 1896; Vaughan and Wells, 1943; Cuif and Dauphin, 1998, 2005). Recently, the terms rapid accretion deposits (RADs) and thickening deposits (TDs) have been substituted for COCs and fibers, respectively (Stolarski, 2003; Nothdurft and Webb, 2007; Brahmi *et al*., 2010; Janiszewska *et al.*, 2011). The RADs formed within the well-differentiated regions of rapid skeletal accretion are enriched in organic components (hollowed-out by acidic etching) (e.g. Brahmi *et al*., 2010). The TDs are skeletal structures deposited outside the areas of rapid accretion and typically consist of fibrous layers continuous with those of the RADs, but poorer in organic components (Brahmi *et al*., 2010). These new terms have been used in this study.

Details of macroskeletal features were observed using optical microscopes (Nikon SMZ-1500; Leica M165C; Leica DM 2700P) and a digital microscope (Keyence VHX-1000). Skeletal microstructures were visualized using scanning electron microscopies (= SEM) (Keyence VE-7000; JEOL JSM-IT100). For SEM observations, transverse or longitudinally polished sections of skeletons were etched for 20–40 s with a 0.1% formic acid solution or cut fragments of skeletons were etched for 30 s with a 10% formic acid solution for observations of heavily etched surface. The sections were rinsed with distilled water and washed in an ultrasonic cleaner for 10–20 s. The samples were mounted on stubs using double-sided adhesive tape and sputter-coated with conductive platinum film.

Results

***Flabellum* (*Flabellum*) *magnificum* Marenzeller, 1904**

Macroskeletal structures

Flabellum (*Flabellum*) *magnificum* shows a flabellate corallum with a smooth calicular edge and no thecal edge spines (Figure 1A, B). Septa show a hexameral arrangement preceded by septal insertions near the two directive septa. The upper calicular edges of the septa are slightly notched but expand below into an exert lobe that extends well into the fossa (Figure 1C, D). The columella is formed by the inner and lower edges of the septa (Figure 1E). *F.* (*F.*) shows a marginothecal wall (*sensu* Stolarski, 1995) with septal furrows on the thecal faces (Figure 1F, G). In particular, the thecal faces corresponding to the septa of S1–S3 are slightly raised to form ridges. Well preserved specimens display thecal faces ornamented with dish-shaped growth lines, looped between the septal furrows (Figure 1G). The most distal parts of the walls show a smooth thecal face without dish-shaped growth lines (Figure 1F). The outer wall of the corallum is not covered with soft tissue and secondary skeletal thickenings. The wall surface is often encrusted and damaged by other skeletozoans and microboring organisms (Figure 1F).

Microskeletal structures

The upper calicular edge of *Flabellum* (*Flabellum*) *magnificum* is smooth at the macroscopic level, whereas the growth peripheral edges of the wall are slightly undulated, when viewed under the microscope (Figure 1D). Both the inner and outer surfaces of the growth edges of the wall are smooth at the margin and about 1 mm wide (Figure 1D, F). The proximal parts of the smooth zone of the wall are covered with growth lines, which are recognized as lined granules (44.4 μm ± 2.7 Mean ± SE, N = 26) (Figure 1F). In contrast, the proximal parts of

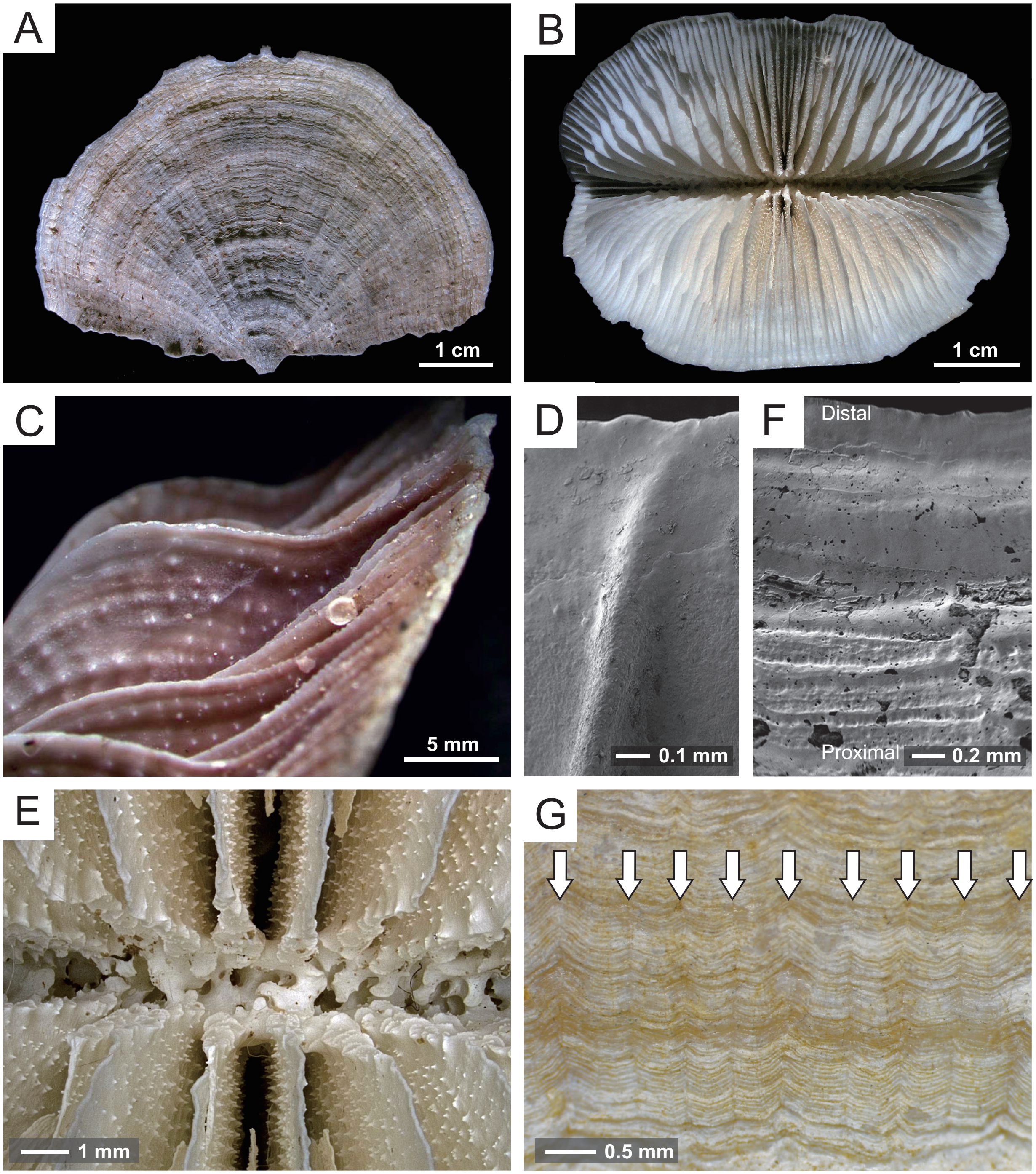

Figure 1. Morphology of *Flabellum* (*Flabellum*) *magnificum*. **A**, side view of a corallum. **B**, distal view of a corallum. **C**, side view of septa. Septal spines are present along the growth lines. **D**, distal part of septum and inner side of wall. The septum grows on inner side of wall. **E**, septal edges and elongated columella in deeper fossa. **F**, most distal parts of the walls show a smooth thecal face (*ca.* 1 mm in width). **G**, close-up view of an outer surface of wall. Dish-shaped growth lines and septal furrows (white arrows) are on the thecal faces.

the smooth surfaces of the inner side of the wall are covered with TD, which have a slightly rough surface with granules.

The polished and etched sections of the distal ends of the walls parallel to the maximum growth direction show dome-shaped strands of RAD, *ca.* 50–100 µm wide (Fig-

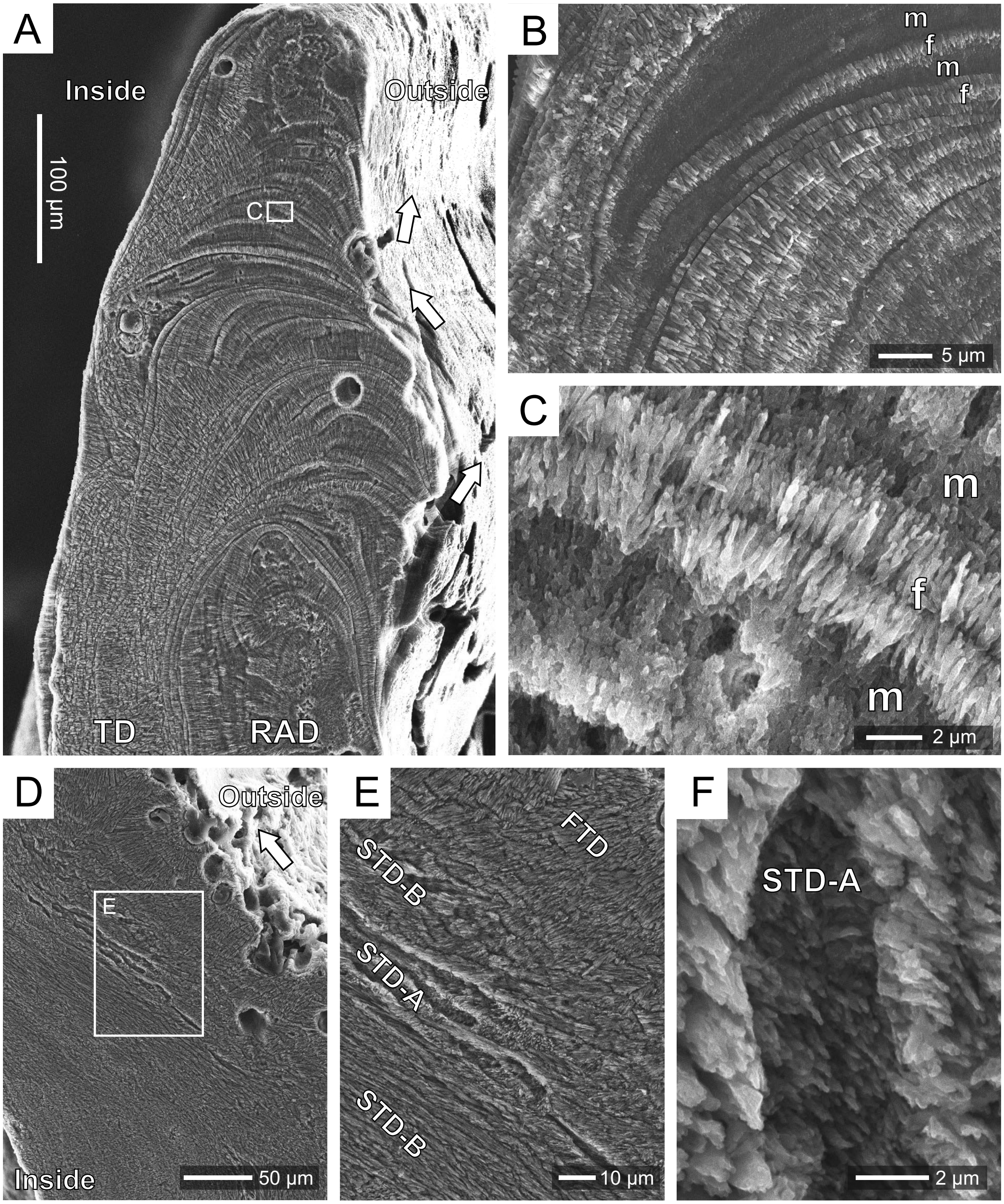

Figure 2. Skeletal microstructures of longitudinal sections of *Flabellum* (*Flabellum*) *magnificum*. **A**, polished and etched section perpendicular to a growth direction of wall showing dome-shaped growth lines of rapid accretion deposits (RAD) and thickening deposits (TD). Arrows indicate growth directions of wall. **B**, enlarged dome-shaped growth lines of RAD which are composed of alternating microcrystalline (m) and fibrous (f) layers. A microcrystalline layer of RAD grades into a fibrous crystal layer. **C**, enlargement of the region in white square in A showing distinct microcrystalline (m) and fibrous (f) layers. **D**, polished and etched section perpendicular to a growth direction of wall. White arrow shows growth direction of RAD. **E**, enlargement of the region in white square in D showing bundles composed of fibrous crystals (= FTD), shingle-like thickening deposits comprised of small crystals and microcrystallines (= STD-A), and shingle-like thickening deposits made up of larger fibers (= STD-B). **F**, enlargement of a STD-A.

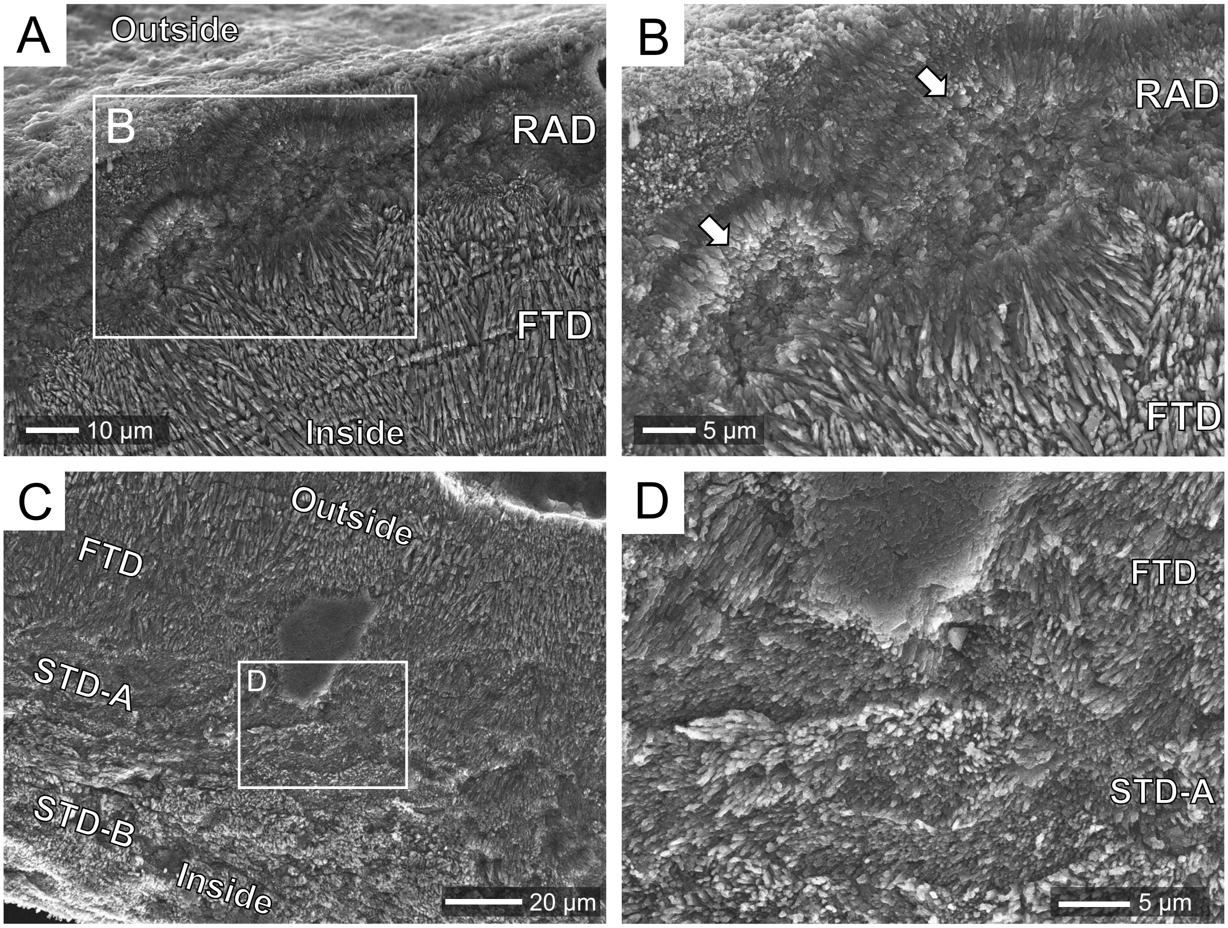

Figure 3. Skeletal microstructures of transverse sections of *Flabellum* (*Flabellum*) *magnificum*. **A**, a transverse section of wall showing laterally continuous RAD zone in outermost part of wall and fibrous thickening deposit (FTD) zones of inner side of the RAD. **B**, enlargement of the region in white square in A showing centers of rapid accretion (CRA; white arrows) in the RAD zone, which are made up of microcrystalline centers and radiating fibers. **C**, a transverse section of TD of the calicular side of the wall showing FTD, STD-A, and STD-B. **D**, enlargement of the region in white square in C showing FTD and STD-A.

ure 2A). The RAD is composed of microcrystalline and fibrous parts, alternately (Figure 2B). The microcrystalline parts of the RAD are aggregates of much smaller nanocrystalline units (up to 1 μm) (Figure 2C). RAD growth direction repeatedly changes inward or outward (Figure 2A). The inner surfaces of the RADs are covered with TDs composed of fibrous crystals (Figure 2A, D–F). The edges of the dome-shaped fibrous layers of the RADs are in some cases continuous with the fibrous parts of the TDs (Figure 2A). The overall growth directions of the wall are identical with the stacking direction of the dome-shaped layers in the RAD. The RAD microcrystalline layers are more developed moving outward from the wall, than moving inward. The thickness of one fibrous crystalline layer of the RAD is unchanged from the center to the side of the layer, whereas a microcrystalline layer of RAD grades into a fibrous crystal layer, especially near the inner face of the wall (Figure 2A, B). No microcrystalline layers are present between the fibrous layers in either the inner or the outer sides of the RAD (Figure 2A). Since microcrystalline layers are formed exclusively in the central part of the RAD, the total growth increments of the central RAD, consisting of microcrystalline and fibrous layers, are larger than those of the RAD sides comprised of only the fibrous layers. TD (stereome) of the calicular side of the wall is divided into three character groups (Figure 2D–F): (1) bundles composed of fibrous crystals (= FTD); (2) shingle-like thickening deposits composed of small crystals and microcrystallines (= STD-A); and (3) shingle-like thickening deposits composed of larger fibers (= STD-B).

The polished and etched sections of the walls perpendicular to the maximum growth direction show laterally continuous RADs at the outermost sections of the walls

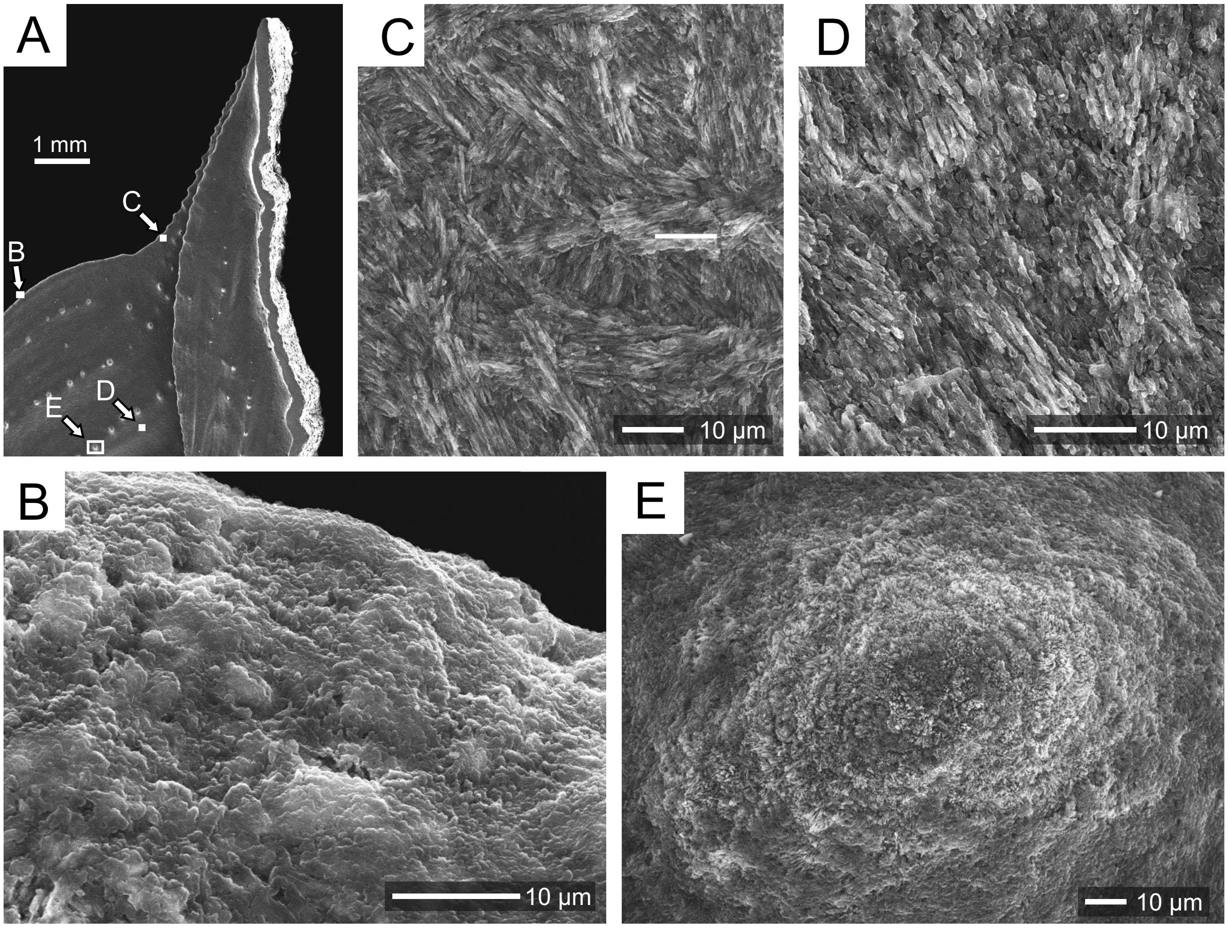

Figure 4. Skeletal microstructures of septa of *Flabellum* (*Flabellum*) *magnificum*. **A**, side view of septa and a wall. **B**, enlarged etched surface of a septal edge in white square in A, which are composed of microcrystallines. **C**, enlarged etched surface of distal part of a septal face in white square in A showing irregular meshwork structures of fibers organized into bundles. **D**, enlarged etched surface of a septal face in white square in A showing fibrous crystals forming shingle-like structures. Longer axis of the fibers is almost uniformly arranged. **E**, enlarged etched surface of a septal spine in white square in A showing microcrystalline deposits.

(Figure 3A, B). The centers of rapid accretion (CRAs), which are made up of microcrystalline centers and radiating fibers, are in some cases shown in the RAD zone (Figure 3B). TD (tectura *sensu* Stolarski, 1995) formed on the outer surface of the RAD is composed of a very thin fibrous, crystalline layer, which is often damaged by microboring (Figure 3A). The TD (stereome) of the calicular side of the wall is divided into three character groups: (1) FTD; (2) STD-A; and (3) STD-B (Figure 3C, D). The bundles of fibrous crystals of FTD, which extend perpendicular to the RAD zone, are often recognized adjacent to the RAD zone. The STDs are formed on the exterior of the layered bundles of the fibrous crystals.

The growth edges of the septa are composed of microcrystallines and show slightly rough surfaces (Figure 4A, B). The septal faces are covered with TDs, which are made up of fibrous crystals forming irregular meshwork structures on distal parts of the septal face and STDs on more proximal parts (Figure 4C, D). Septal spines are composed of microcrystallines (Figure 4E). Transverse sections of septa show RAD in the mid-septal zone and TD on both sides of the RAD. The septal RAD consists of a series of CRA in the mid-septal zone. The TD adjacent to the septal RAD is comprised of layers of fibers orientated almost perpendicular to the septal surface. The TD near the septal surfaces shows individually flattened and elongated bundles of fibers oriented at a low angle to the basal RAD plane, showing shingle-like appearances.

***Flabellum* (*Ulocyathus*) *deludens* Marenzeller, 1904**

Macroskeletal structures

The corallum is slightly compressed flabellate with jagged calicular edges (Figure 5A, B). The proximal parts of the corallum often attach to sand particles. Columel-

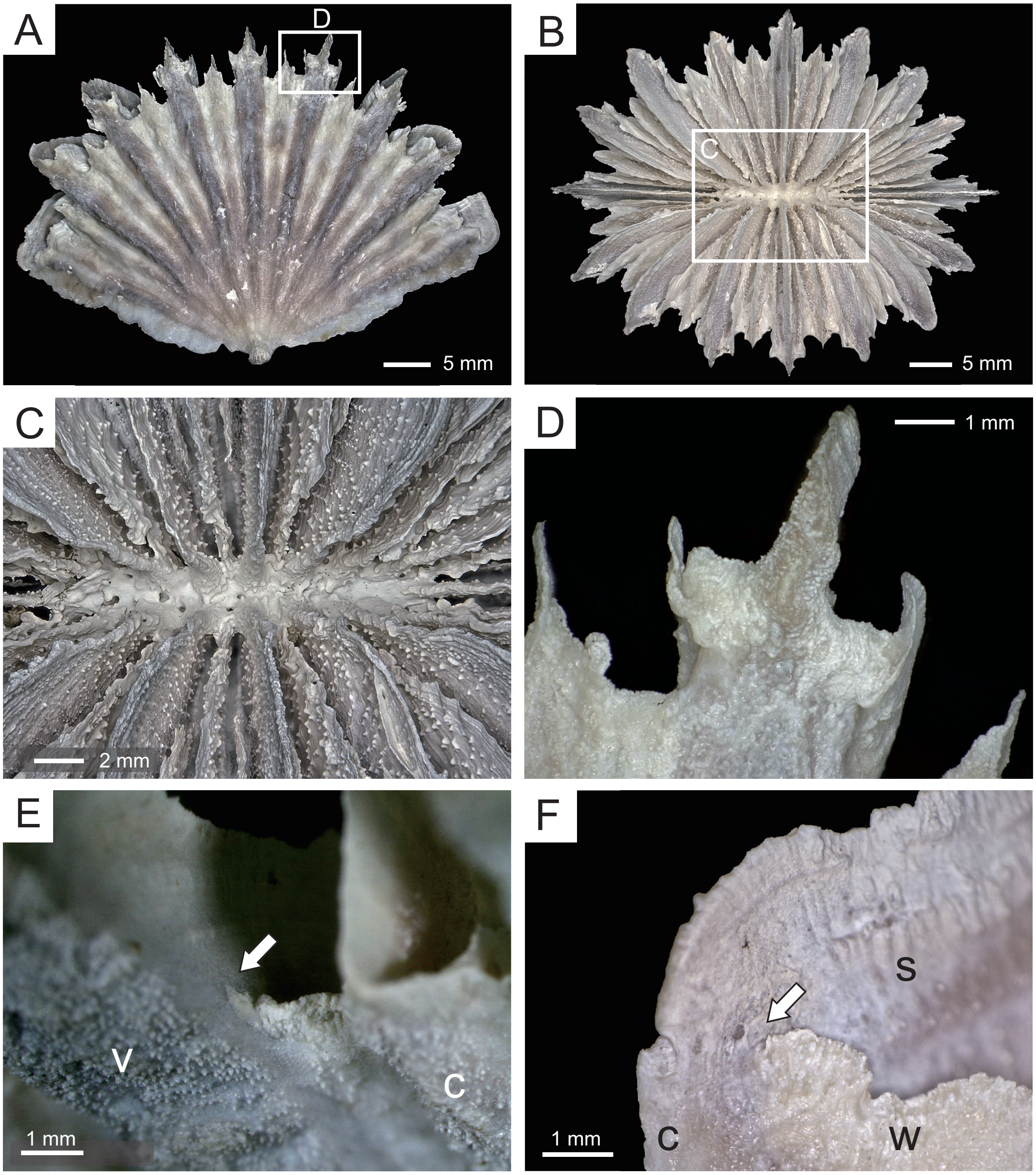

Figure 5. Morphology of *Flabellum* (*Ulocyathus*) *deludens*. **A**, side view of a corallum. **B**, distal view of a corallum. **C**, close-up view of septal edges and fossa shown in white square in B. **D**, close-up view of walls and septa in convex part of a calicular edge shown in white square in A. **E**, a boundary between convex (v) and concave (c) parts of a calicular edge. A wall of concave part is attached to septal faces of the 4th cycle of a septum (white arrow). **F**, directive septum (s) and costa (c). Wall (w) crawls up on slightly inner part of septal face (white arrow). The costa is covered by secondary skeletal deposits.

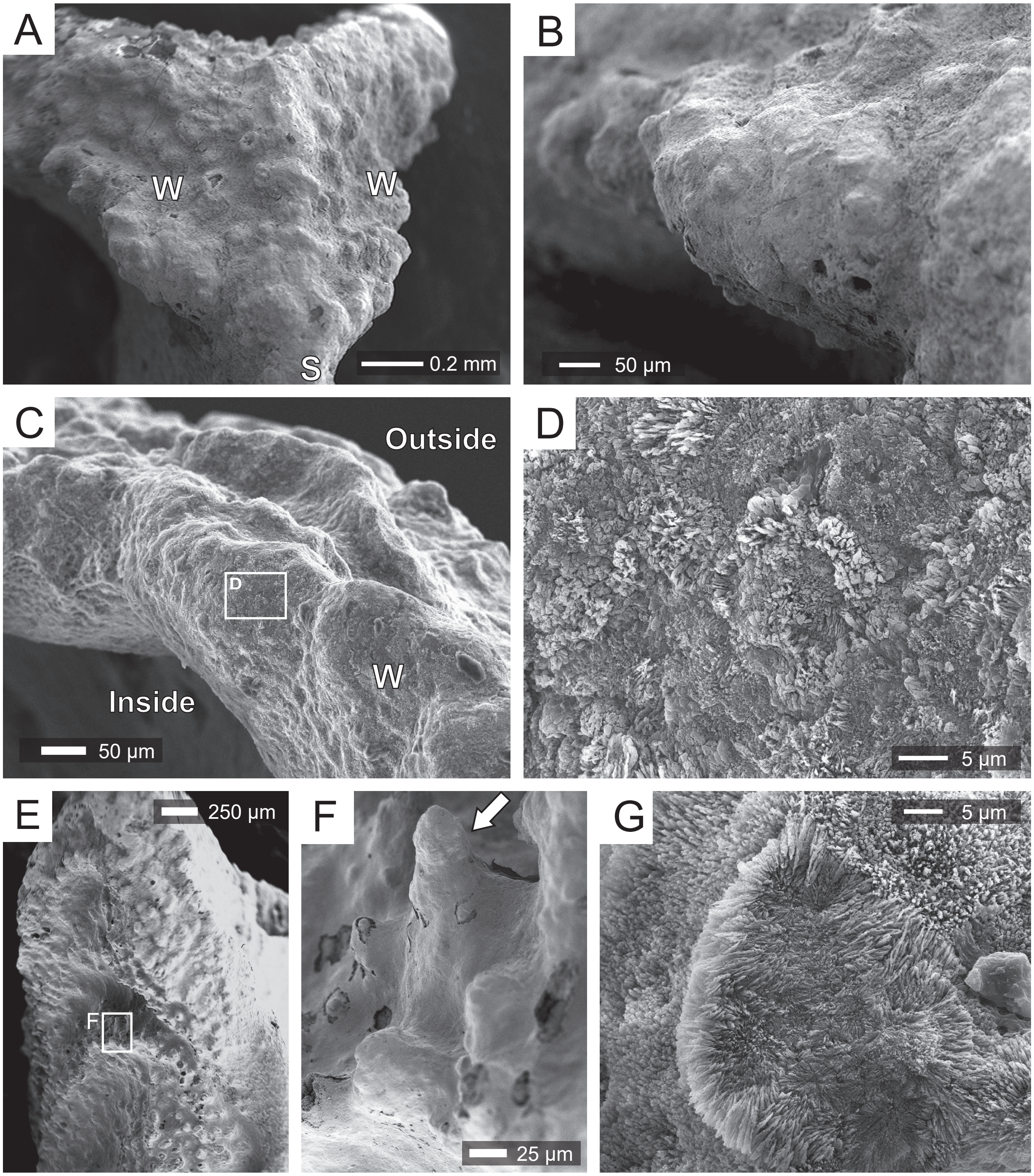

Figure 6. Skeletal microstructures of growth edge of walls of *Flabellum* (*Ulocyathus*) *deludens*. **A**, most distal part of a septum (s) and walls (w) of convex part of calicular edges. **B**, close-up view of growth edge of the wall showing very rough surfaces with small granules. **C**, etched growth edge of a wall (w) in convex part of calicular edges. **D**, enlarged etched surface of a wall in white square in C showing radial small fibrous crystallines and microcrystallines. **E**, outer wall surfaces in a convex part of calicular edge. Small, lined granules on the wall surface form growth lines. **F**, close-up view of a pillar structure (white arrow) of a tubercle shown in white square in E. **G**, broken, etched part of the pillar structure composed of gathered CRAs and layered, small fibrous crystals.

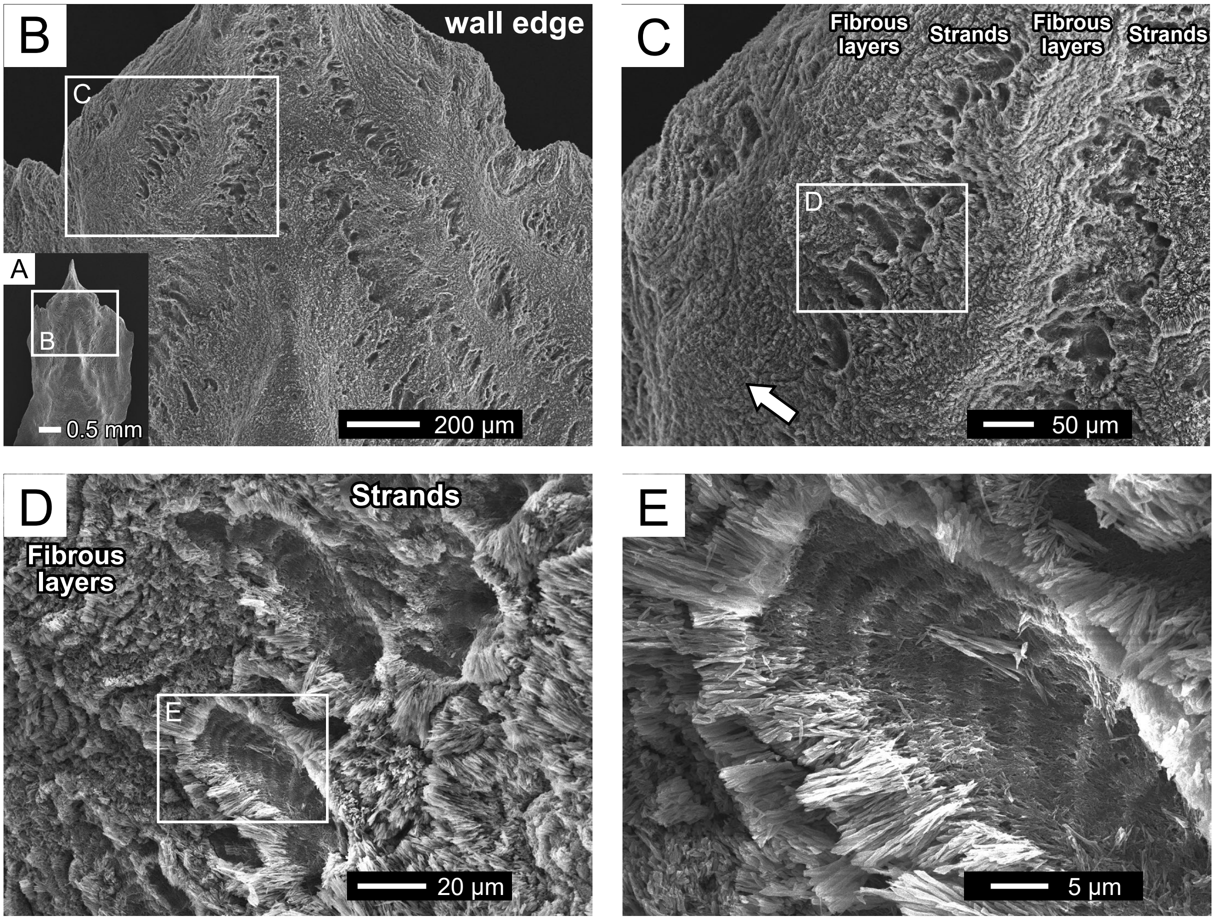

Figure 7. Etched outer surface of wall of *Flabellum* (*Ulocyathus*) *deludens*. **A**, outer surface of convex part of wall. **B**, enlarged etched outer surface of the upper part of wall in white square in A showing growth lines almost parallel to wall edges. **C,** enlargement of the region in white square in B showing alternated strands and fibrous layers. White arrow indicates growth direction of the strands. **D**, close-up view of strands in white square in C. Strands are arranged side by side, and surrounding fibrous layers are composed of short fibers approximately 2–5 μm long. **E**, enlargement of the region in white square in D showing a strand composed of very short fibers (*ca.* 0.5–5 μm long) or microcrystallines with meniscus structure.

lae are formed by the fusion of spiny projections growing from the axial edges of the septa (Figure 5C).

F. (*U.*) *deludens* forms tent-like walls in the jagged, convex parts, where either the 1st or the 2nd cycles of the septa and its adjacent 4th cycle are bridged by concurrent walls (Figure 5A, D). The 3rd cycle of the septa and the adjacent 4th cycle form a concave area. The walls of these concavities link the septal faces of the 4th cycle and the 3rd cycle on the convex area (Figure 5E). Outer surfaces of the walls are covered with small, lined granules, especially on the convex portions (Figure 5D). Two directive septa form distinct costae on both thecal edges and are secondarily covered by calcareous deposits (= tectura). The growing wall crawls up on the inner parts of the directive septal faces (Figure 5F). The costae are covered with secondary skeletal deposits.

Microskeletal structures

The growth edges of the wall often show very rough surfaces with lined tubercles (*ca.* 100–200 μm in diameter) formed by small CRAs (*ca.* 3–20 μm in diameter), which are composed of microcrystallines in the central part of the CRA and radial, small fibrous crystallines in its peripheral part (Figure 6A–D). The tubercles occasionally form a pillar structure composed of gathered CRAs that is covered with layered, small fibrous crystals in its peripheral part (Figure 6E–G).

The heavily etched outer surface of the wall shows alternated strands (*sensu* Stolarski, 2003) and fibrous layers (Figure 7A–C). A strand corresponding to CRAs of RAD is approximately 50–100 μm long and 20–30 μm wide composed of very short fibers (*ca.* 0.5–5 μm long) or microcrystallines with meniscus structure (Figure

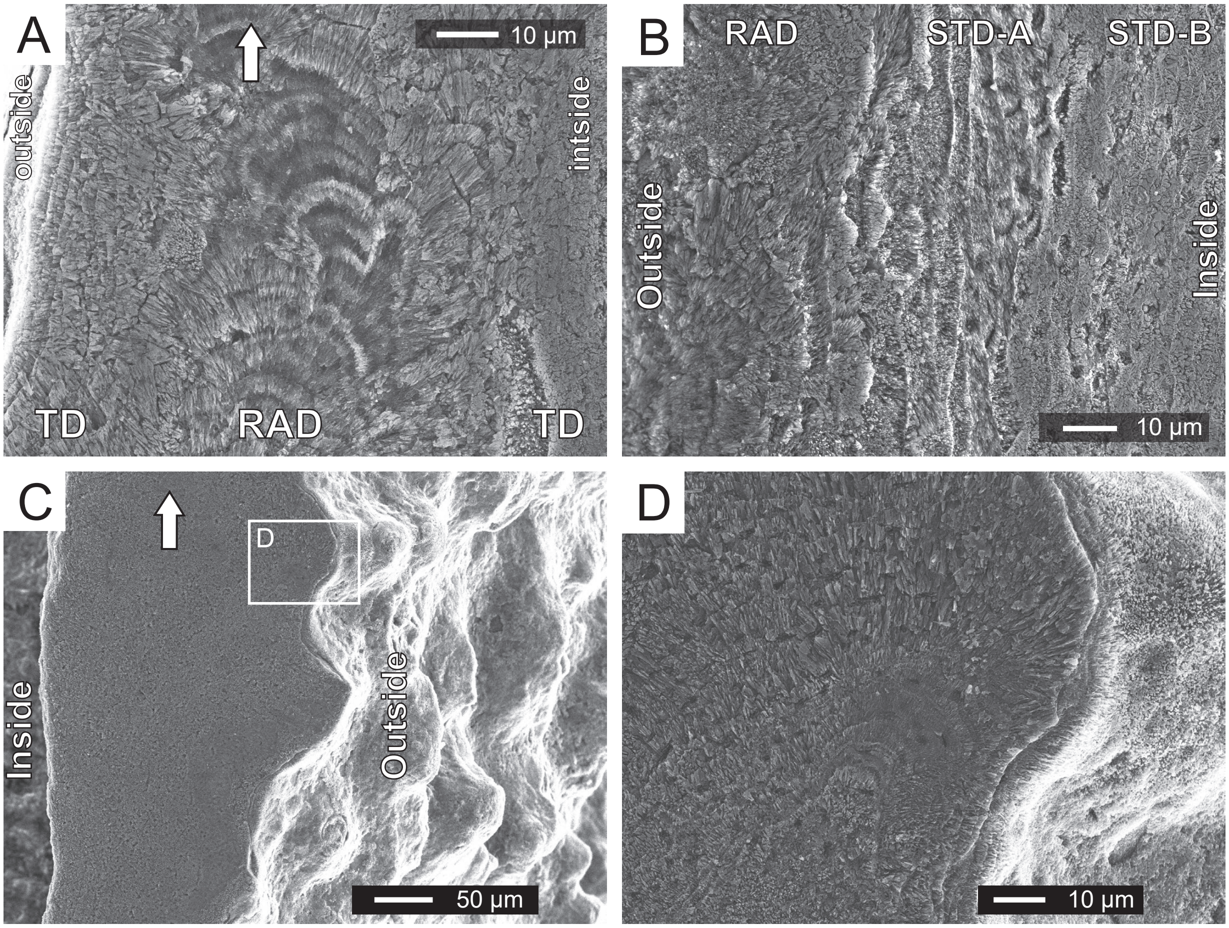

Figure 8. Skeletal microstructures of *Flabellum* (*Ulocyathus*) *deludens*. **A**, longitudinal polished and etched sections quasi-parallel to the maximum growth direction of a strand showing RAD composed of strand of small fibers and TDs with thin fibrous layers. White arrow indicates growth direction of wall. **B**, longitudinal polished and etched sections of an inner part of wall showing RAD and TDs. The TD of the calicular side of the walls are composed of shingle-like thickening deposits consisting of small crystals and microcrystalline (= STD-A) and shingle-like thickening deposits made up of larger fibers (= STD-B). **C**, longitudinal polished and etched sections showing alternated strands and fibrous layers. White arrow indicates maximum growth direction of the wall. **D**, close-up view of the strand and fibrous layers shown in white square in C showing strand and dome-shaped fibrous layers.

7D, E). Each strand is covered with thin fibrous layers composed of short fibers growing perpendicular to the outer line of the strand (Figure 7D, E). The strands are arranged side by side along the growth line of the wall. Growth direction of the strands is obviously oblique to maximum growth direction of the wall or septum (Figure 7C, D). Especially, growth direction of the wall, which is close to the 1st or 2nd cycle of septa, in its convex part is almost perpendicular to the septal surface. In contrast, the strands that are close to the 4th cycle, in the convex part of wall are almost parallel to the septa. The fibrous layers are composed of short fibers approximately 2–5 µm long.

In the polished and etched sections of the walls quasi-parallel to the maximum growth direction of a strand, the RADs are composed of alternated strands and fibrous layers (Figure 8). Each strand often shows arch-shaped growth lines. The strand zone is covered with dome-shaped fibrous layers (Figure 8C, D).

The polished and etched sections of the walls perpendicular to the maximum growth direction of the strand show slightly continuous RADs in the outer parts of the walls (Figure 9A). The CRAs, which are made up of microcrystalline central parts and radiating fibers, are in some cases shown in the RAD zones (Figure 9B). The CRAs show a slightly scattered arrangement in the RAD zones and correspond to the strand recognized in the longitudinal sections (Figure 9B). TDs are present in both the outer and inner parts of the RAD in the wall. Thin fibrous layers of TDs (= tectura) are recognized in the outermost parts of the walls (Figure 9A). The fibrous lay-

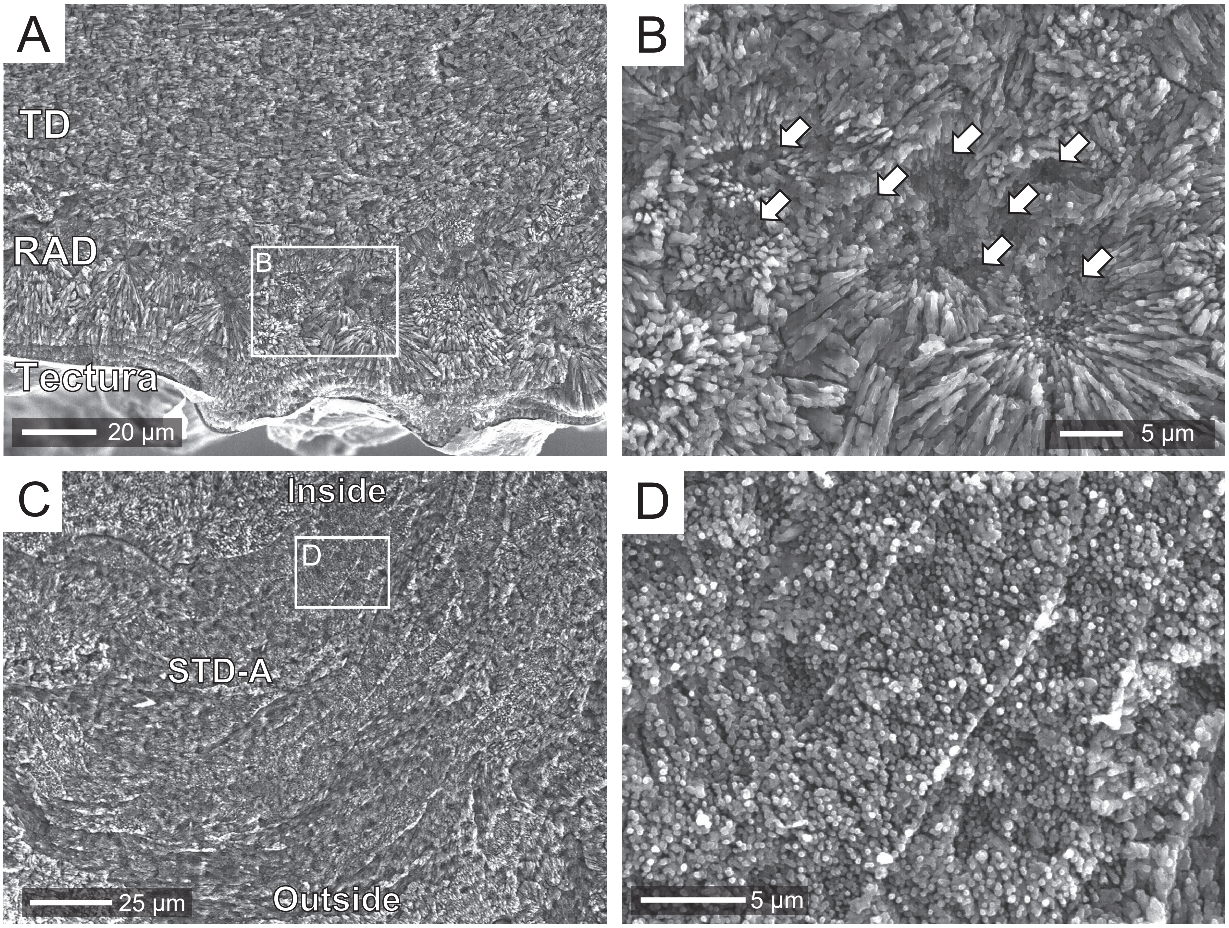

Figure 9. Skeletal microstructures of *Flabellum* (*Ulocyathus*) *deludens*. **A**, polished and etched transverse sections of an outer part of wall showing TD and laterally continuous RAD zone. **B**, close-up view of the center of rapid accretions (= CRA) (white arrows) in white square in A showing a slightly scattered arrangement in the RAD zone. **C**, transverse polished and etched sections of an inner side of wall located at the corner of a 1st cycle septum and a wall showing thick STD-A zones. **D**, close-up view of STD-As composed of microcrystallines shown in white square in C.

ers are also covered with a projection that originates from a strand in the RAD zone.

The TD (= stereome) of the calicular side of the walls is divided into two characteristic groups (Figures 8B, 9C, D): (1) shingle-like thickening deposits composed of small crystals and microcrystalline (= STD-A) (Figures 8B, 9C, D); (2) shingle-like thickening deposits composed of larger fibers (= STD-B) (Figure 8B). Thick STD-A zones are in many cases recognized around the corners of 1st and 2nd cycles of septa and walls.

The growth edges of the septa, made up of microcrystallines, show smooth to slightly rough surfaces (Figure 10A, B). Septal faces are covered with irregular meshwork formed by small fibers or STDs (Figure 10C). The longer axes of the fibers of meshwork and STDs are almost parallel to the septal face.

The polished and etched sections of the septa perpendicular to the septal face show RADs in the central area (Figure 10D, E). The RADs are covered with a meshwork of fibers consisting of small fibers quasi-parallel to the septal faces and STDs. The meshwork of fibers is especially evident near the RAD zone.

Discussion

Growth edges of the walls

The growth edges of the walls of *Flabellum* in this study show two patterns: (1) smooth surfaces in *F.* (*F.*) *magnificum* (Figures 1D, F, 2A), and (2) pronounced rough and nodular surfaces in *F.* (*Ulocyathus*) *deludens* (Figure 6A, B). The surface morphologies of the growth edges are closely related to the characteristics of the RADs on the walls and their inner structures (Figures 2A, 6C, D). Smooth or slightly smooth surfaces at the growth edges

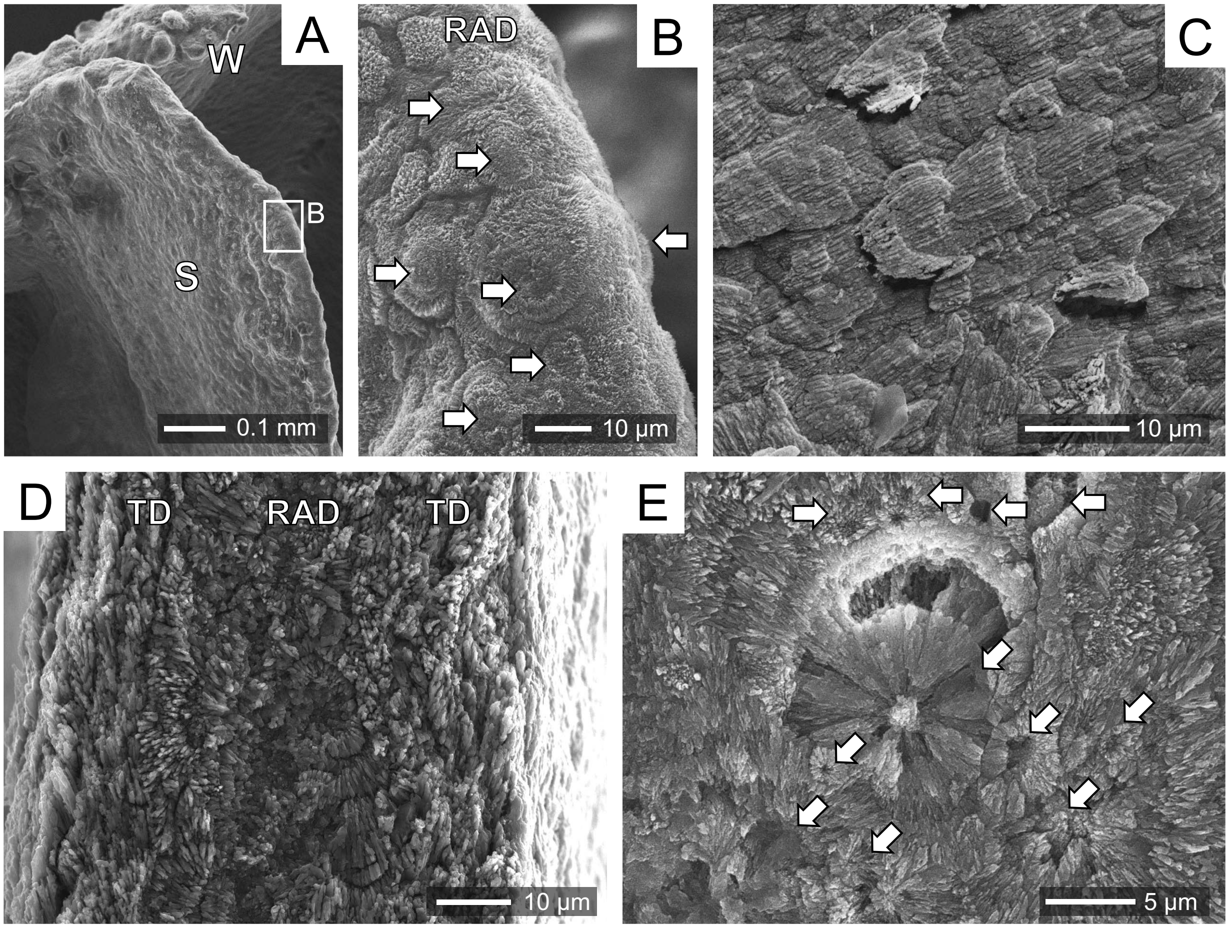

Figure 10. Skeletal microstructures of septa of *Flabellum* (*Ulocyathus*) *deludens*. **A**, distal part of a wall (w) and septum (s). **B**, close-up view of etched growth edge of a septum in white square in A showing a smooth to slightly rough surface and CRAs (white arrows) which show a slightly scattered arrangement in a continuous RAD zone. **C**, etched surface of a septal face showing fibrous crystals forming shingle-like structures. The longer axes of the fibers are almost parallel to the septal face. **D**, polished and etched transverse sections of a septum showing RAD and TDs. The RAD composed of gathered CRAs form a continuous mid-septal zone. **E**, close-up view of the CRAs (white arrows) of the RAD of septum made up of small fibrous crystallines showing a slightly scattered arrangement in the RAD zone.

of the walls show continuously dome-like growth in the longitudinal sections of the RAD (Figure 2A). In contrast, a rough surface at the growth edges corresponds to piled-up, discrete strand and dome-like fibrous layers (Figure 7A). The RAD structures of *F*. (*U*.) *deludens* are influenced by subtle differences in skeleton secretion rates at the growth edge surfaces between the tubercles (strands) at the microscopic level (Figure 6A, B).

Most flabellids show laterally continuous walls at the calicular edges (Cairns, 1989). In contrast, the walls of *F*. (*U*.) *deludens* are not continuous laterally, being divided into convex and concave parts (Figure 5A, D, E). Particularly, the species has costae only at the two directive septa (Figure 5F). Full-grown *Javania cailleti* also shows distinct costae corresponding to the 1st to 3rd cycles of septa (Stolarski, 1995), whereas *F*. (*U*.) *deludens* forms costae only at the two corallum edges from a very early growth stage.

RAD of the walls

A longitudinal section of the RAD of the walls of *Flabellum* (*Flabellum*) *magnificum* shows a dome-shaped morphology composed of microcrystalline and fibrous layers (Figure 2A–C). The same feature is also found in other scleractinians (Wise, 1972; Jell, 1974; Jell and Hill, 1974; Stolarski, 2003; Nothdurft and Webb, 2007; Brahmi *et al.*, 2010; Janiszewska *et al.*, 2011). In flabellids, *Truncatoflabellum spheniscus* and *Rhizotrochus typus* also show dome-shaped RAD morphology (Tokuda and Ezaki, 2013). Relative thickness of the microcrystalline and fibrous layers in the continuous RAD zone varies, even within the same specimen (Figure 2A, B).

The fibrous layers of the RAD are formed without microcrystalline layers along the sides of the walls, even if the microcrystalline layers are present in the central areas between the two fibrous layers (Figure 2A, B). This result suggests discontinuous or minimum skeletal growth between the two fibrous layers in the sides of the walls, at least during the growth of the microcrystalline zone in the central parts of the RADs. In addition, these microcrystalline layers are predominant in the outward growing part of the wall (Figure 2A). Barnes (1972) assumed that the outward and inward growths of the wall in *Manicina areolata* were produced by daily changes in the shape of the secreting polypal tissue. Our results clearly show that relative thickness, composition, and growth direction of the microcrystalline and fibrous layers of the RAD in *F.* (*F.*) *magnificum* are influenced not only by genetic factors, but also by extrinsic factors (e.g. ambient environmental fluctuations and resultant metabolic activities of polyps).

F. (*U*.) *deludens* shows digitated strands and dome-like fibrous layers in a longitudinally sectioned RAD (Figure 8A). This type of RAD in the wall structure is totally different from that of the other flabellid species [*F.* (*F.*) *magnificum*, *T. spheniscus*, and *R. typus*].

Skeletal microstructures are controlled by a genetically coded organic matrix (Janiszewska *et al.*, 2011). The secretions of granular and fiber-like aragonite in the skeleton are clearly involved with the production of Galaxin and Amgalaxin-like molecules, respectively (Reyes-Bermudez *et al.*, 2009). The morphologies of the fibrous and microcrystalline crystals are common among the flabellids. However, the resulting compositions and morphologies of the units composed of fibers and microcrystallines are totally different in *Flabellum* (*Flabellum*) and *Flabellum* (*Ulocyathus*). These results indicate that the growth and pattern formations of the crystals constituting the skeletons may be controlled by not only the types of organic matrices, but also the three-dimensional spatial distributions of the organic matrices and the timings of secretion.

TDs of the walls

The TDs of the inner parts of the walls (= stereome) of *Flabellum* include three characteristic types, as below: (1) bundles of fibrous crystals oriented more or less perpendicular to the RAD surfaces [*Flabellum* (*Flabellum*) *magnificum*, Figure 2A, E] (= FTD), (2) shingle-like structure composed of microcrystallines [*F*. (*F*.) *magnificum*, Figure 2A, E; *F.* (*Ulocyathus*) *deludens*, Figures 8B, 9C, D] (= STD-A), (3) shingle-like structure composed of fibers [*F*. (*F*.) *magnificum*, Figure 2D, E; *F*. (*U*.) *deludens*, Figure 8B] (= STD-B). In contrast, *F*. (*F*.) *magnificum* and *F*. (*U*.) *deludens* show fibrous layers of TD in the outer edge of the wall's RAD (tectura; Figure 3A, B). However, *F*. (*U*.) *deludens* shows a thicker TD layer than *F*. (*F*.) *magnificum* (Figure 8A). *F.* (*F.*) therefore differs from *F.* (*U*.) in having a fibrous layer of TD in the inner side of the RAD and thinner tectura. Although Acroporidae is not closely related to Flabellidae according to molecular phylogeny, shingle-like surface textures of the TDs are also observed in *Acropora* (Wallace, 1999; Nothdurft and Webb, 2007; Stolarski *et al.*, 2016).

STD-A of *F*. (*U*.) *deludens* is formed directly along the inner surfaces of RAD (Figure 8B). Growth rates of the microcrystalline parts are higher than those of the fibrous parts (e.g. RAD vs. TD; Brahmi *et al.*, 2012). In *F*. (*U*.) *deludens* having slightly light and thin coralla, the microcrystalline of the STD-A may contribute to rapid skeletal growth of walls rather than increasing their thickness and strength. A variety of thicknesses of the microcrystalline zones in places indicate that the formation of the TDs is strongly affected by physiological mechanisms.

Septal microstructures

Septal microstructures have been analyzed in various scleractinian corals in order to understand their taxonomic characteristics in relation to molecular phylogeny (e.g. Stolarski, 2003; Budd and Stolarski, 2009). Stolarski (2003) proposed a "layered model of the septal growth (covering of TD around the RAD at the growing periphery)", which has been slightly modified and updated by Nothdurft and Webb (2007) and Janiszewska *et al.* (2011). Septa of *Flabellum* (*Flabellum*) *magnificum* and *Flabellum* (*Ulocyathus*) *deludens* show the same RAD microskeletal morphology, following the layered model of septal growth (*sensu* Stolarski, 2003). In contrast, a new septal growth model of TDs is required for the two subgenera of *Flabellum*, both exhibiting shingle-like TDs. Both subgenera show (1) irregularly arranged bundles of fibers; (2) STD-A composed of microcrystalline; and (3) STD-B made up of fibers. The irregularly meshwork of fibers has also been recognized in the septal TD of micrabaciid corals (Janiszewska *et al.*, 2011). However, those fibers are much shorter in length than those of *Flabellum*. In addition, irregularly arranged TDs are covered by shingle-like TDs in the later growth stages. Structures of the septal TDs are thus changed according to their growth stages and/or sites of formation of the corallites.

Comparison of microskeletal characters with molecular phylogeny

Flabellum is characterized by its free-living flabellate corallum showing no transverse division. Cairns (1989) divided *Flabellum* into two subgenera, *Flabellum* (*Flabellum*) having a smooth calicular edge, and *Flabellum* (*Ulocyathus*) having a jagged one. Molecular phylogenetic analysis indicates that *F*. (*U*.) *deludens* and *F*. (*U*.) *japonicum* form a distinct cluster. *F*. (*F*.) *magnificum* and *F*. (*F*.) *pavoninum* form another distinct cluster, which is closely related to *Monomyces pygmaea* (Tokuda *et al*., 2010). Skeletal microstructures of the walls of *F.* (*U.*) *deludens* are totally different from those of *F.* (*F.*) *magnificum* in regard to RAD (digitated strand and dome-shaped fibrous layer vs. continuous dome-shaped alternation) and TD characteristics. Moreover, *F.* (*U.*) shows a laterally discontinuous wall and costae in the corallum edges. These microskeletal differences support the results of molecular phylogeny. However, *F*. (*F*.) *impensum* does not belong to the same cluster as *F*. (*F*.) *magnificum* and *F*. (*F*.) *pavoninum*, although they have similar corallite characters (i.e. flabellate corallum, smooth calicular edge). Interestingly, *F*. (*F*.) *impensum* is closely linked with the cluster of *F*. (*U*.) *deludens* and *F*. (*U*.) *japonicum*, contrary to its placement in the traditional classification. *F*. (*F*.) *impensum* exhibits a flabellate corallum with a smooth calicular edge like *F*. (*F*.) *magnificum* and *F*. (*F*.) *pavoninum* (Tokuda *et al*., 2010). Microskeletal characteristics of other species of *Flabellum* are to be elucidated in near future for the understanding of overall flabellid evolution.

Acknowledgments

We thank Takashi Matsuda (Port of Nagoya Public Aquarium) and Yoshitsugu Kaji (Wakayama Prefectural Museum of Natural History) for providing us with specimens. We are also grateful to Takamoto Okudaira (Osaka City University) for his help in the SEM analysis. This work was supported by Tottori University of Environmental Studies Grant-in-Aid for Special Research and Tottori Prefecture Environmental Research Grant. This research was also supported by grants from the Scientific Research Fund of the Japan Society for the Promotion of Science (21340154, 22654062, 26400503, 15H03744, 16K13898, 18K13649). We are grateful to two anonymous reviewers for their useful comments on the manuscript.

References

Barnes, D. J., 1972: The structure and formation of growth-ridges in scleractinian coral skeletons. *Proceedings of the Royal Society of London*, *Series B*, vol. 182, p. 331–350.

Benzoni, F., Arrigoni, R., Stefani, F., Reijnen, B. T., Montano, S. and Hoeksema, B. W., 2012: Phylogenetic position and taxonomy of *Cycloseris explanulata* and *C. wellsi* (Scleractinia: Fungiidae): lost mushroom corals find their way home. *Contributions to Zoology*, vol. 81, p. 125–146.

Benzoni, F., Stefani, F., Stolarski, J., Pichon, M., Mitta, G. and Galli, P., 2007: Debating phylogenetic relationships of the scleractinian *Psammocora*: molecular and morphological evidences. *Contributions to Zoology*, vol. 76, p. 35–54.

Bourne, G. C., 1887: The anatomy of the madreporarian coral *Fungia*. *Quarterly Journal of Microscopical Science*, vol. 27, p. 293–324.

Brahmi, C., Domart-Coulon, I., Rougée, L., Pyle, D. G., Stolarski, J., Mahoney, J. J., Richmond, R. H., Ostrander, G. K. and Meibom, A., 2012: Pulsed ^{86}Sr-labeling and NanoSIMS imaging to study coral biomineralization at ultra-structural length scales. *Coral Reefs*, vol. 31, p. 741–752.

Brahmi, C., Meibom, A., Smith, D., Stolarski, J., Auzoux-Bordenave, S., Nouet, J., Doumenc, D., Djediat, C. and Domart-Coulon, I., 2010: Skeletal growth, ultrastructure and composition of the azooxanthellate scleractinian coral *Balanophyllia regia*. *Coral Reefs*, vol. 29, p. 175–189.

Budd, A. F. and Stolarski, J., 2009: Searching for new morphological characters in the systematics of scleractinian reef corals: comparison of septal teeth and granules between Atlantic and Pacific Mussidae. *Acta Zoologica*, vol. 90, p. 142–165.

Cairns, S. D., 1989: A revision of the ahermatypic Scleractinia of the Philippine islands and adjacent waters. *Smithsonian Contributions to Zoology*, vol. 486, p. 1–136.

Cairns, S. D., 1999: Species richness of recent Scleractinia. *Atoll Research Bulletin*, vol. 459, p. 1–12.

Cairns, S. D., 2016: A key to the genera and species of the transversely-dividing Flabellidae (Anthozoa, Scleractinia, Flabellidae), with a guide to the literature, and the description of two new species. *Zookeys*, vol. 562, p. 1–48.

Cairns, S. D., 2017: New azooxanthellate genus of Scleractinia (Flabellidae) from the Australian Cenozoic. *Journal of Paleontology*, vol. 91, p. 407–416.

Cuif, J.-P. and Dauphin, Y., 1998: Microstructural and physico-chemical characterization of 'centers of calcification' in septa of some Recent scleractinian corals. *Paläontologische Zeitschrift*, vol. 72, p. 257–269.

Cuif, J.-P. and Dauphin, Y., 2005: The two-step mode of growth in the scleractinian coral skeletons from the micrometre to the overall scale. *Journal of Structural Biology*, vol. 150, p. 319–331.

Cuif, J.-P., Lecointre, G., Perrin, C., Tillier, A. and Tillier, S., 2003: Patterns of septal biomineralization in Scleractinia compared with their 28S rRNA phylogeny: a dual approach for a new taxonomic framework. *Zoologica Scripta*, vol. 32, p. 459–473.

Fukami, H., Budd, A. F., Paulay, G., Solé-Cava, A., Chen, C. A., Iwao, K. and Knowlton, N., 2004: Conventional taxonomy obscures deep divergence between Pacific and Atlantic corals. *Nature*, vol. 427, p. 832.

Fukami, H., Chen, C. A., Budd, A. F., Collins, A., Wallace, C., Chuang, Y.-Y., Chen, C., Dai, C.-F., Iwao, K., Sheppard, C. and Knowlton, N., 2008: Mitochondrial and nuclear genes suggest that stony corals are monophyletic but most families of stony corals are not (Order Scleractinia, Class Anthozoa, Phylum Cnidaria). *PLoS ONE*, 3(9), e3222, doi:10.1371/journal.pone.0003222.

Janiszewska, K., Stolarski, J., Benzerara, K., Meibom, A., Mazur, M., Kitahara, M. V. and Cairns, S. D., 2011: A unique skeletal microstructure of the deep-sea micrabaciid scleractinian corals. *Journal of Morphology*, vol. 272, p. 191–203.

Jell, J. and Hill, D., 1974: The microstructure of corals. *Ancient Cnidaria*, vol. 1, p. 8–14.

Jell, J. S., 1974: The microstructure of some scleractinian corals. *Proceedings of the 2nd International Coral Reef Symposium, Brisbane*, vol. 2, p. 301–320.

Kitahara, M. V., Cairns, S. D., Stolarski, J., Blair, D. and Miller, D. J., 2010: A comprehensive phylogenetic analysis of the Scleractinia (Cnidaria, Anthozoa) based on mitochondrial CO1 sequence data. *PLoS ONE*, 5(7), e11490, doi:10.1371/journal.pone.0011490.

Kitahara, M. V., Stolarski, J., Cairns, S. D., Benzoni, F., Stake, J. L. and

Miller, D. J., 2012: The first modern solitary Agariciidae (Anthozoa, Scleractinia) revealed by molecular and microstructural analysis. *Invertebrate Systematics*, vol. 26, p. 303–315.
Le Goff-Vitry, M. C., Rogers, A. D. and Baglow, D., 2004: A deep-sea slant on the molecular phylogeny of the Scleractinia. *Molecular Phylogenetics and Evolution*, vol. 30, p. 167–177.
Marenzeller, E. von., 1904: Steinkorallen. *In*, Chun C. *ed.*, *Wissenschaflichte Ergebnisse der deutschen Tiefsee-Expedition auf dem Dampfer "Valdivia"*, *1838–1899*, vol. 7, p. 261–318. Gustav Fischer Verlag, Jena.
Nothdurft, L. D. and Webb, G. E., 2007: Microstructure of common reef-building coral genera *Acropora*, *Pocillopora*, *Goniastrea* and *Porites*: constraints on spatial resolution in geochemical sampling. *Facies*, vol. 53, p. 1–26.
Ogilvie, M. M., 1896: Microscopic and systematic study of madreporarian types of corals. *Philosophical Transactions of the Royal Society B: Biological Sciences*, vol. 187, p. 83–345.
Reyes-Bermudez, A., Lin, Z., Hayward, D. C., Miller, D. J. and Ball, E. E., 2009: Differential expression of three galaxin-related genes during settlement and metamorphosis in the scleractinian coral *Acropora millepora*. *BMC Evolutionary Biology*, vol. 9, doi:10.1186/1471-2148-9-178.
Romano, S. and Cairns, S. D., 2000: Molecular phylogenetic hypotheses for the evolution of scleractinian corals. *Bulletin of Marine Science*, vol. 67, p. 1043–1068.
Romano, S. L. and Palumbi, S. R., 1996: Evolution of scleractinian corals inferred from molecular systematics. *Science*, vol. 271, p. 640–642.
Sorauf, J. and Podoff, N., 1977: Skeletal structure in deep water ahermatypic corals. *Mémoires du Bureau de recherches géologiques et minières*, vol. 89, p. 2–11.
Stolarski, J., 1995: Ontogenetic development of the thecal structures in caryophylliine scleractinian corals. *Acta Palaeontologica Polonica*, vol. 40, p. 19–44.
Stolarski, J., 1996: Gardineria—a scleractinian living fossil. *Acta Palaeontologica Polonica*, vol. 41, p. 339–367.
Stolarski, J., 2003: Three-dimensional micro-and nanostructural characteristics of the scleractinian coral skeleton: a biocalcification proxy. *Acta Palaeontologica Polonica*, vol. 48, p. 497–530.
Stolarski, J., Bosellini, F. R., Wallace, C. C., Gothmann, A. M., Mazur, M., Domart-Coulon, I., Gutner-Hoch, E., Neuser, R. D., Levy, O., Shemesh, A. and Meibom, A., 2016: A unique coral biomineralization pattern has resisted 40 million years of major ocean chemistry change. *Scientific Reports*, 27579, doi:10.1038/srep27579.
Stolarski, J., Kitahara, M. V., Miller, D. J., Cairns, S. D., Mazur, M. and Meibom, A., 2011: The ancient evolutionary origins of Scleractinia revealed by azooxanthellate corals. *BMC Evolutionary Biology*, vol. 11, doi:10.1186/1471-2148-11-316.
Tokuda, Y. and Ezaki, Y., 2013: Attachment structures in *Rhizotrochus* (Scleractinia): macro- to microscopic traits and their evolutionary significance. *Lethaia*, vol. 46, p. 232–244.
Tokuda, Y., Ikeno, T., Goto, S. G., Numata, H. and Ezaki, Y., 2010: Influence of different substrates on the evolution of morphology and life-history traits of azooxanthellate solitary corals (Scleractinia: Flabellidae). *Biological Journal of the Linnean Society*, vol. 101, p. 184–192.
Vaughan, T. W. and Wells, J. W., 1943: Revision of the Suborders Families, and Genera of the Scleractinia. *Geological Society of America Special Papers*, vol. 44, p. 1–394.
Wallace, C., 1999: *Staghorn corals of the world: a revision of the genus Acropora*, 421 p. CSIRO publishing, Melbourne.
Wise, S., 1972: Observations of fasciculi on developmental surfaces of scleractinian coral exoskeletons. *Biomineralization*, vol. 6, p. 160–175.

Author contributions

Y. T. designed and performed all the experiments. Y. T. and Y. E. analysed the results and wrote the manuscript. All authors gave final approval for publication.